EUROPHYSICS LETTERS 1 October 2005

Europhys. Lett., **72** (1), pp. 96–102 (2005)
DOI: 10.1209/epl/i2005-10202-4

Towards the phase diagram of a polydisperse mixture of charged hard spheres

Yu. V. Kalyuzhnyi[1], G. Kahl[2] and P. T. Cummings[3,4]

[1] *Institute for Condensed Matter Physics - Svientsitskoho 1, 79011 Lviv, Ukraine*
[2] *Center for Computational Materials Science and Institut für Theoretische Physik TU Wien - Wiedner Hauptstraße 8-10, A-1040 Wien, Austria*
[3] *Department of Chemical Engineering, Vanderbilt University Nashville, TN 37235-1604, USA*
[4] *Chemical Sciences Division, Oak Ridge National Laboratory Oak Ridge, TN 27831-6110, USA*

received 17 May 2005; accepted in final form 29 July 2005
published online 31 August 2005

PACS. 64.10.+h – General theory of equations of state and phase equilibria.
PACS. 64.70.Fx – Liquid-vapor transitions.
PACS. 61.20.Qg – Structure of associated liquids: electrolytes, molten salts, etc.

Abstract. – In an effort to approach a *quantitative* determination of the phase diagram of polydisperse mixtures of (possibly size-asymmetric) charged hard spheres (CHS), we propose a concept that explicitly takes into account the association of the ions into dimers, *i.e.*, an effect that is known to be of high relevance close to the liquid-vapor phase boundary in the restricted primitive model (RPM). We use the polymer mean spherical approximation (PMSA) to calculate the properties of this polydisperse mixture of dimers. The concept turns out to be a truncatable free energy model, thus the phase diagram can be calculated by solving a highly non-linear set of equations. We present the full phase diagram (in terms of cloud and shadow curves and binodals) and discuss fractionation effects for a model system.

Introduction. – The critical point of the restricted primitive model (RPM) for electrolytes, *i.e.*, a binary mixture of oppositely charged hard spheres (CHS), was believed to exist over a long time [1,2]. However, it was verified only in the 1970s when both Monte Carlo (MC) simulations [3, 4] and statistical-mechanics–based theories [5, 6] provided confirming results (for an overview see [7]). Ever since, considerable effort has been dedicated to a *quantitatively* reliable description of the coexistence curve and, in particular, to an exact location of the critical point of the RPM. Meanwhile, computer simulations have provided —as a consequence of significant progress in methodological and computational developments— a highly accurate picture [8–11]. On the other hand, results obtained in theoretical concepts are less satisfactory: standard liquid-state theories either do not converge in regions sufficiently close to the critical point [12], or predict —as, *e.g.*, the mean spherical approximation (MSA)— critical parameters that differ by a factor of ∼1.6 in temperature and ∼0.2 in density from simulation data. Only recently [13–17], could significant improvement of these values be achieved: these sophisticated concept, are based on the meanwhile well-established fact [15, 18–23] that close to the phase boundaries the RPM is characterized by a high degree of ionic association, *i.e.*, its properties are dominated by the presence of neutral clusters, while the amount of free

© EDP Sciences
Article published by EDP Sciences and available at http://www.edpsciences.org/epl or http://dx.doi.org/10.1209/epl/i2005-10202-4

ions or charged clusters is negligible. And indeed, inclusion of these effects has brought along a substantial improvement over simple approaches (such as the MSA): now results differ from the "exact" simulation data for the critical point only by a factor of $\sim$1.3 in temperature and $\sim$0.6 in density. In these studies it was assumed that all the clusters formed upon association in the system are represented by so-called minimal size neutral clusters (MSNC), *i.e.*, dimers in the case of 1 : 1 model, trimers in the case of 1 : 2 model, etc. These clusters were then treated within the framework of the polymer MSA (PMSA) [15, 21, 22].

The RPM represents undoubtedly a suitable model for electrolytes or molten salts. For fluids of charged *mesoscopic* particles (such as macromolecules, colloids, or micelles), however, the RPM is a rather idealized model, since it does not consider polydispersity, *i.e.*, a characteristic feature of colloidal suspensions, which is —as a consequence of the production process— omnipresent in such systems. Thus, a polydisperse mixture of CHS would represent a more appropriate model. Unfortunately, for theoreticians this brings along considerable complications: compared to monodisperse systems, computer simulations are now disproportionately more expensive and successful theoretical concepts that are able to predict the phase behavior on a *quantitative* level are up to date rather rare. Still, it is highly desirable to have detailed information about the phase diagram of such a system: academic interest will certainly focus on polydispersity as such, which leads to an intriguing phase behavior and phase transitions, and fractionation effects [24]; technology, on the other hand, will rather be interested in realistic polydisperse charged systems, such as the ones mentioned above.

In this letter we present a new and comprehensive concept that captures the two particular features of polydisperse mixtures of CHS in an appropriate manner and thus offers a route towards a *quantitative* determination of the phase diagram: it takes explicitly into account both the polydisperse character of the mixture as well as ionic association effects.

We view a polydisperse system as a mixture with a (formally) infinite number of components, each characterized by a continuous species index x. The amount of each species x is defined via the distribution function $f(x)$, which is positive and normalized, *i.e.*, $\int_0^\infty \mathrm{d}x f(x) = 1$. $f(x)\mathrm{d}x$ is the fraction of particles with species index $\bar{x} \in [x, x + \mathrm{d}x]$. The main problem to determine the phase behavior of polydisperse mixtures lies in the fact that the Helmholtz free energy is now defined in a space of infinite dimensionality, where the coexistence equations have to be solved. Recent contributions have demonstrated that the concept of truncatable free-energy models [24] represents one of the few (conceptually and numerically) viable routes out of this dilemma [25, 26]: here the free energy can be expressed by a finite (but large) number of generalized moments of $f(x)$, mapping thus the infinitely many coexistence equations onto a finite set of relations. To cope with the association effects, we have generalized the concept of MSNC to polydisperse mixtures of CHS which is treated within the PMSA [15, 21, 22]. The model turns out to be a truncatable free-energy model; although the resulting framework is rather intricate, it offers for the first time access to the *full* phase diagram (in terms of cloud and shadow curves and binodals) of a polydisperse mixture of CHS.

Our model includes a possible size asymmetry, while it is restricted (at least at present) to the charge-symmetric case; in this sense the present contribution is preliminary. Inclusion of asymmetry in charge would lead to formation of n-mers ($n \geq 3$) which would require a considerably more complex formalism. For the future we plan to use our MSNC concept to study polydisperse models of highly asymmetric electrolyte solutions (*i.e.*, mixtures of large and highly charged polydisperse macroions and monodisperse small counterions) generalizing the corresponding solution of the PMSA presented in [27].

With the present concept we realize two goals: i) we pass the level of the MSA (that we have used recently in [28]), which, being a linear theory, is definitely unsuited to treat strongly interacting systems; ii) despite its conceptual and numerical complexity the present concept

offers the possibility of *systematic* investigations of the phase behavior of polydisperse mixtures of CHS, something which is —at least at present— out of reach for computer simulations, as they require an increased computational effort of one or two orders of magnitude and therefore can only be applied to isolated systems [29]. In this letter we present the first results; for a detailed presentation of the rather complex formalism we refer to [30].

Model and theory. – We consider a polydisperse mixture of CHS, *i.e.*, a polydisperse generalization of the 1 : 1 size-asymmetric electrolyte primitive model (PM). The species of the particles are characterized by two continuous variables, the charge z and the size σ. Assuming additivity in size, *i.e.*, $\sigma_{12} = (\sigma_1 + \sigma_2)/2$, two particles of the species (σ_1, z_1) and (σ_2, z_2) interact via

$$\Phi(r; \sigma_1, z_1, \sigma_2, z_2) = \begin{cases} \infty, & r \leq \sigma_{12}, \\ e^2 z_1 z_2 / \epsilon r, & \sigma_{12} < r \leq \infty. \end{cases} \tag{1}$$

The particles are immersed in a dielectric continuum with a dielectric constant ϵ at temperature T; further, $\beta = 1/k_{\mathrm{B}}T$ and $\beta^* = e\beta/\epsilon$. The number density of the system is $\rho = \rho_+ + \rho_-$ and the system is neutral. z and σ are distributed according to a positive, normalized distribution function; in an effort to keep the conceptual and numerical effort within reasonable limits we make the physically sound choice that the charge of the particles is proportional to their surface, *i.e.*, $z_\pm(\sigma) = \pm\sigma^2/\langle\sigma^2\rangle_\pm$, where $\langle\sigma^2\rangle_\pm$ is the second moment of the distribution function; we are thus left with σ as the only continuously distributed variable. Introducing $\langle\sigma\rangle_\pm = \int_0^\infty \mathrm{d}\sigma\sigma f_\pm(\sigma)$ with $\langle\sigma\rangle_- = \tau\langle\sigma\rangle_+$, we assume for the distribution functions of the positively and negatively charged particles $f_+(\sigma) = f(\sigma)$ and $f_-(\sigma) = \tau^{-1} f(\sigma/\tau)$ so that the average charge is $\langle z\rangle_\pm = \int_0^\infty \mathrm{d}\sigma z_\pm(\sigma) f_\pm(\sigma) = \pm 1$.

We investigate the two-phase equilibrium of a polydisperse mixture of CHS: at a given temperature T the mother phase, characterized by the distribution functions $f_\pm^{(0)}(\sigma)$ and the number density $\rho^{(0)}$, separates into two coexisting daughter phases, with distribution functions $f_\pm^{(k)}(\sigma)$ and densities $\rho^{(k)}$, $k = 1, 2$. The superscripts denote the properties of the respective phases: 1 stands for the low-density (gas) phase and 2 for the high-density (liquid) phase.

Generalizing the concept of MSNCs to the polydisperse case, we now have to consider a polydisperse mixture of neutral dimers formed by two oppositely CHS with the size ratio τ. PMSA [21, 22] is certainly an appropriate tool to calculate the thermodynamic properties of this system, which will then be required to determine phase equilibrium. The solution of the PMSA for a multicomponent mixture of CHS [21, 22] can be reduced to the solution of one single non-linear equation for the scaling parameter, Γ. These expressions are readily generalized to the polydisperse case, replacing the discrete set of concentrations by the continuous distribution function and summations over discrete species indices become integrations over the distribution function. For the mother phase, with $f(\sigma) = f^{(0)}(\sigma)$, this equation reads

$$\Gamma^2 = \pi\beta^*\rho \int_0^\infty \mathrm{d}\sigma\, f(\sigma) \left\{ \frac{1}{2} \sum_\alpha Z_\alpha^2 \Gamma_\alpha^2 + \frac{\Gamma_+ + \tau\Gamma_-}{1+\tau} \prod_\alpha Z_\alpha \Gamma_\alpha \right\}, \tag{2}$$

where the index α takes the values $-$ or $+$; further $\Gamma_\alpha \equiv \Gamma_\alpha(\sigma) = [1 + (\delta_{\alpha+} + \tau\delta_{\alpha-})\sigma\Gamma]^{-1}$, $Z_\alpha \equiv Z_\alpha(\sigma) = \alpha z - (\delta_{\alpha+} + \tau\delta_{\alpha-})\sigma\Lambda$, $z \equiv z(\sigma) = z_+(\sigma)$, $\Lambda = \pi D/(2\Delta + \pi\Omega)$, $\Delta = 1 - \pi\zeta_3/6$,

$$\zeta_m = \frac{1}{2}\rho(1+\tau^m) \int_0^\infty \mathrm{d}\sigma\sigma^m f(\sigma), \qquad D = \frac{1}{2}\rho \int_0^\infty \mathrm{d}\sigma f(\sigma)\sigma z[\Gamma_+ - \tau\Gamma_- - (1-\tau)\Gamma_{\Pi}],$$

$$\Omega = \frac{1}{2}\rho \int_0^\infty \mathrm{d}\sigma f(\sigma)\sigma^3 \left(\Gamma_+ + \tau^3\Gamma_- + \frac{2\tau^2}{1+\tau}\Gamma_{\Pi} \right),$$

and $\Gamma_\Pi = \Gamma_+\Gamma_-$. Similar relations hold for the Γ's of the daughter phases, introducing the yet unknown functions $f^{(k)}(\sigma)$, $k = 1, 2$. Note that for the present model we have $f_+^{(k)}(\sigma) = f^{(k)}(\sigma)$ and $f_-^{(k)}(\sigma) = \tau^{-1} f^{(k)}(\sigma/\tau)$ ($k = 0, 1, 2$). For details see [30].

Knowing the Γ's for each of the phases, we follow Bernard and Blum [31,32] and present expressions for the excess (over ideal gas) pressure and chemical potential, ΔP and $\Delta\mu(\sigma)$:

$$\beta\Delta P = \beta\Delta P^{(\mathrm{HS})} - \frac{1}{6}\pi\lambda_1\zeta_3 - \frac{1}{4}\pi\lambda_2\zeta_2\left(1 + \frac{\pi\zeta_3}{3\Delta}\right) - \frac{\Gamma^3}{3\pi} - \frac{2\beta^*}{\pi}\Lambda^2, \tag{3}$$

$$\begin{aligned}\beta\Delta\mu(\sigma) \;=\; & \beta\left[\Delta\mu^{(\mathrm{HS})}(\sigma) + \Delta\mu^{(\mathrm{HS})}(\tau\sigma)\right] - \ln\left[\frac{1}{\Delta}\left(\frac{\pi\zeta_2}{2\Delta}\frac{\tau\sigma}{1+\tau} + 1\right)\right] - \\ & -\frac{1}{6}\pi\sigma^2\left[\frac{3}{2}\lambda_2(1+\tau^2) + \sigma(1+\tau^3)\Big(\lambda_1 + \frac{\pi}{2\Delta}\zeta_2\lambda_2\Big)\right] - \beta^*\left\{z^2\left[\Gamma\Gamma_\Sigma + \frac{2\Gamma_\Pi}{(1+\tau)\sigma}\right] - \right. \\ & \left. - 2z\Lambda[z\Gamma_\Sigma - \Gamma_\Pi(1-\tau)\sigma] - \Lambda^2\sigma^3\left[\Gamma_+ + \tau^3\Gamma_- + \frac{2\tau^2\Gamma_\Pi}{1+\tau} - \frac{1}{3}(1+\tau^3)\right]\right\},\end{aligned} \tag{4}$$

$$\lambda_n = \frac{1}{2}\,\rho\int_0^\infty \mathrm{d}\sigma f(\sigma)\frac{(1+\tau)\delta_{n1} + 2\tau\sigma\delta_{n2}}{(1+\tau)\Delta + \frac{1}{2}\pi\sigma\tau\zeta_2}, \qquad n = 1, 2, \tag{5}$$

where $\Gamma_\Sigma = \Gamma_+ + \Gamma_-$. The corresponding properties of the reference system, *i.e.*, a polydisperse mixture of uncharged hard-sphere (HS) dimers ($\Gamma = 0$), are calculated via Wertheim's thermodynamic perturbation theory [33, 34]; $\Delta P^{(\mathrm{HS})}$ and $\Delta\mu^{(\mathrm{HS})}(\sigma)$ are the excess pressure and chemical potential of a HS system, which are calculated using the semiempirical expressions due to Mansoori *et al.*, generalized to the polydisperse case [26]. Those thermodynamic properties which we require to calculate phase equilibrium depend at given temperature $T^* = 1/\beta^*$, and given $\rho^{(0)}$ and $f_\pm^{(0)}(\sigma)$, only on a finite set of generalized moments of $f_\pm^{(0)}(\sigma)$.

Equilibrium conditions require conservation of the total volume and of the total number of particles of each species. Further, the truncated free-energy concept guarantees that the (formally) infinitely many coexistence equations (*i.e.*, $P^{(1)} = P^{(2)}$ and $\mu^{(1)}(\sigma) = \mu^{(2)}(\sigma)$ for all σ) are mapped onto a set of 18 coupled, highly non-linear equations (see [30]); for each phase we have seven unknown generalized moments $\{\zeta_1, \zeta_2, \zeta_3, \lambda_1, \lambda_2, D, \Omega\}$, and, in addition, ρ and Γ; once they are determined, the $f_\pm^{(k)}(\sigma)$, $k = 1, 2$, are calculated following a scheme developed earlier [25, 26, 28]. The equations are solved with a Newton-Raphson–based algorithm.

As explained in [26] we have used a Beta-distribution function for the mother phase, which is specified by three parameters [26,28]: the average size of the particles, $\sigma_0 = \langle\sigma\rangle_+^{(0)}$, the width, $D_0 = \langle\sigma^2\rangle_+^{(0)}/\sigma_0^2 - 1$, and the cut-off diameter of the distribution function, $\sigma_\pm^{\max} = 2\langle\sigma\rangle_+^{(0)}$.

Results. – We present results for a specific system which is a generalization of the 1 : 1 size-asymmetric electrolyte PM characterized by $\sigma_+^{\max} = 2\sigma_0$, $\sigma_-^{\max} = 2\tau\sigma_0$, $D_0 = 0.01$, and $\tau = 0.7$. In fig. 1 we show the liquid-gas phase diagram; it includes the cloud and shadow curves, along with three binodals for three selected densities, one of them being the critical density $\rho_{\mathrm{cr}}^* = \rho_{\mathrm{cr}}\sigma_0^3 = 0.102$. For reference we also display the binodal curve for the (bidisperse) PM calculated within the PMSA [15] (fig. 1a) and the MSA data for the polydisperse system (fig. 1b). Comparison between the bidisperse and the polydisperse CHS fluid shows that polydispersity shifts the critical point to higher densities and to higher temperatures: $\rho_{\mathrm{cr}}^* = 0.102$, $T_{\mathrm{cr}}^* = 0.086$ in the polydisperse case, while $\rho_{\mathrm{cr},PM}^* = 0.076$, $T_{\mathrm{cr},PM}^* = 0.076$ in the case of the bidisperse mixture (PM). Comparison between PMSA and MSA for the polydisperse system points out that the strong asymmetry in the MSA results

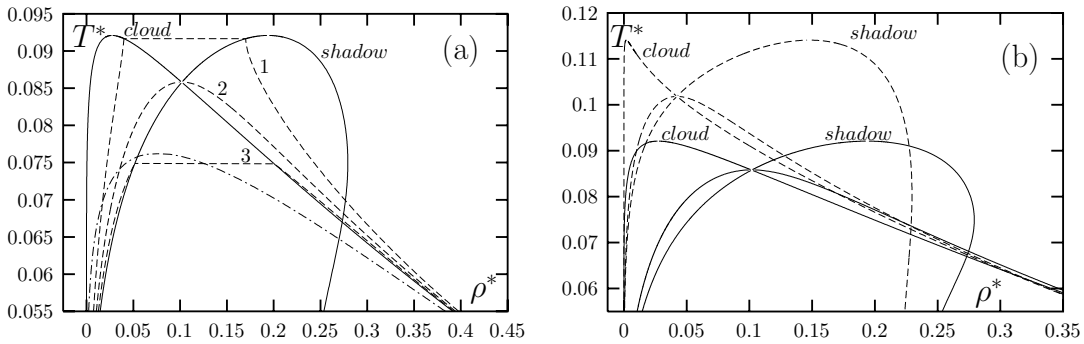

Fig. 1 – Phase diagram of a polydisperse mixture of CHS with $\tau = 0.7$. (a) Cloud and shadow curves (solid lines); binodals: broken lines are for $\rho^{(0)*} = 0.04(1), 0.102(2), 0.2(3)$; the dashed-dotted line is for bidisperse PM with $\tau = 0.7$; (b) MSA [28] (dashed lines) and PMSA (solid lines) phase diagrams.

for the cloud curve is taken away; as a consequence of the association effects the critical temperature is decreased while the critical density becomes larger. In fig. 2 we study the influence of size asymmetry and of polydispersity on the location of the critical point and display $T^*_{\rm cr}$ and $\rho^*_{\rm cr}$ as functions of τ for two values of D_0, *i.e.* $D_0 = 0$ (bidisperse case) and $D_0 = 0.01$; results are calculated within PMSA and MSA. We have also added MC simulation data for the PM [35, 36], which is the limiting case as $D^{(0)} \to 0$; similar results for finite polydispersity, *i.e.*, $D^{(0)} > 0$, are not available in the literature. Both MSA and PMSA are able to describe the increase of $T^*_{\rm cr}$ and $\rho^*_{\rm cr}$ with the decrease of τ (*i.e.*, increase of the size asymmetry) for τ-values down to $\sim$0.33 and $\sim$0.23, respectively. As τ is further decreased, simulation predicts a decrease in $T^*_{\rm cr}$ and in $\rho^*_{\rm cr}$, while the corresponding MSA- and PMSA-curves continue to increase. In the entire range of τ-parameter, MSA gives too high values for $T^*_{\rm cr}$ and too low values for $\rho^*_{\rm cr}$: this is a consequence of the fact that MSA is not able to describe ionic association properly. PMSA, on the other hand, is able to take ionic association into account, at least on the level of complete dimerization; this modification substantially improves MSA results: $T^*_{\rm cr}$ is shifted to lower values and $\rho^*_{\rm cr}$ to higher values, respectively, approaching thus, at least for the bidisperse case ($D^{(0)} = 0$), the simulation data. At this point we add an —admittedly— rather speculative remark: due to the lack of simulation data for the critical point in polydisperse CHS mixtures, we estimate —based on the MSA and the PMSA data for the polydisperse case and on simulation data for the 1 : 1 PM— the location for the critical point of a polydisperse CHS mixture in simulation (see fig. 2, open squares) as a function of the size asymmetry parameter τ in the range $0.33 \leq \tau \leq 1.0$. Based on this extrapolation, we expect that both $T^*_{\rm cr}$ and $\rho^*_{\rm cr}$ will increase in this range with decreasing τ.

Leaving a more detailed discussion of the daughter distribution functions, $f^{(k)}(\sigma)$, $k = 1, 2$, to a later contribution [30], we focus here rather on a quantitative analysis of fractionation effects: we consider the respective first moments, $\langle\sigma\rangle^{(k)}_{\pm}$, which give information about the size-distribution of the particles and on the widths, $D^{(k)}_{\pm}$, in the daughter phases, indicating the degree of polydispersity; for their definitions we refer to [26]. From the $\langle\sigma\rangle^{(k)}_{\pm}$ (fig. 3a), we observe that along the shadow curve fractionation has its strongest effect: smaller particles prefer to be in the gas phase, while the larger ones are predominantly encountered in the fluid phase. Note that these effects are stronger for subcritical densities, while for supercritical densities $\langle\sigma\rangle^{(k)}_{\pm} \sim \langle\sigma\rangle^{(0)}_{\pm}$. The width of the $f^{(k)}_{\pm}(\sigma)$ —fig. 3b— show a distinctively different behavior than in the MSA [28] where for all temperatures $D^{(k)}_{\pm} < D^{(0)}_{\pm} (= 0.01)$: for densities

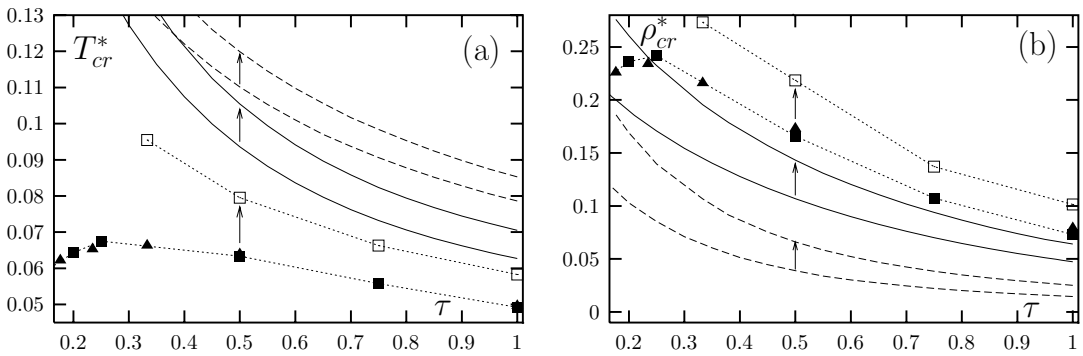

Fig. 2 – $T^*_{\rm cr}$ (a) and $\rho^*_{\rm cr}$ (b) *vs.* $\tau = \langle\sigma\rangle_-/\langle\sigma\rangle_+$ for polydisperse mixture of CHS at $D_0 = 0$ (bidisperse mixture, lower lines) and $D_0 = 0.01$ (polydisperse mixture, upper lines), as predicted by MSA (dashed lines), PMSA (solid lines), and the extrapolation scheme (open squares, see text); MC simulations (filled triangles [35] and filled squares [36]) only for the bidisperse case. Arrows indicate how the critical parameters vary as D_0 changes from 0 to 0.01.

below the critical density and for higher temperatures, $D^{(2)}_\pm$ can exceed in the fluid phase the values of $D^{(0)}_\pm$; for this parameter range the $f^{(2)}_\pm(\sigma)$ of the fluid phase are broadened with respect to the $f^{(0)}_\pm(\sigma)$. In addition, for $\rho^* < \rho^*_{\rm cr}$, and for lower temperatures, $D^{(1)}_\pm < D^{(2)}_\pm$, while at higher temperatures, $D^{(1)}_\pm > D^{(2)}_\pm$, leading to a loop-like shape of the $D^{(k)}_\pm$-curves (broken line in fig. 3b). A particularly non-monotonic behavior is observed for the values of $D^{(k)}_\pm$ along the shadow curve, which is in distinct contrast to the MSA results.

Conclusions. – With the concept presented above we are able to calculate the full phase diagram of a polydisperse, possibly size-asymmetric mixture of CHS, taking into account association effects on the level of dimers. For a particular system we have discussed the phase diagram and fractionation effects. By varying the polydispersity and the size asymmetry of the system we are able to predict how the location of the critical point will vary with these parameters. With this contribution we hope to encourage computer simulation experts to perform similar investigations and to test the reliability of the data we have predicted.

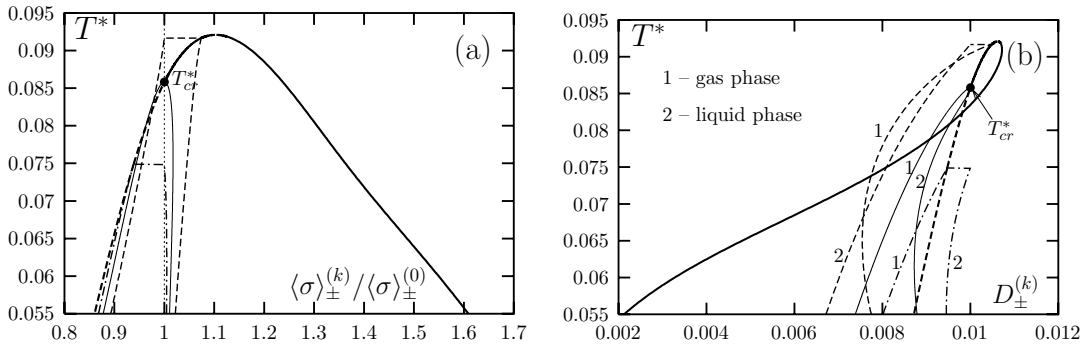

Fig. 3 – First moment, $\langle\sigma\rangle^{(k)}_\pm$ (a), and width, $D^{(k)}_\pm$ (b), of the daughter distribution functions $f^{(k)}_\pm(\sigma)$ as discussed in the text for the polydisperse mixture of CHS along the binodals for the parent phase densities $\rho^{(0)*} = 0.04$ (broken line), $\rho^{(0)*} = \rho^*_{\rm cr} = 0.102$ (full line), $\rho^{(0)*} = 0.2$ (dash-dotted line), and along the shadow curve (thick full and thick broken line). In (a) the dotted vertical line through $\langle\sigma\rangle^{(k)}_\pm/\langle\sigma\rangle^{(0)}_+ = 1$ separates the gas (left) from the fluid (right) region.

* * *

This work was supported by the Österreichischer Forschungsfonds (FWF) under Proj. Nos. P14371, P15785, and P17823 and by the BMBWK under Proj. No. GZ 45.492/1-VI/B/7a/2002. YVK gratefully acknowledges the hospitality at the CMS and the Institut für Theoretische Physik at the TU Wien, where part of this work was performed.

REFERENCES

[1] McQuarry D. A., *J. Phys. Chem.*, **66** (1962) 1508.
[2] Stillinger F. H. and Lovett R., *J. Chem. Phys.*, **48** (1968) 3858.
[3] Vorontsov-Veliaminov N. P., El'yashevich A. M., Morgenshtern L. A. and Chasovskikh V. P., *Teplofiz. Vys. Temp.*, **8** (1970) 277.
[4] Chasovskikh V. P. and Vorontsov-Veliaminov P. N., *High Temp. (USSR)*, **14** (1976) 174.
[5] Ebeling W., *Z. Phys. Chem.*, **247** (1971) 340.
[6] Stell G., Wu K. C. and Larsen B., *Phys. Rev. Lett.*, **37** (1976) 1369.
[7] Weingärtner H. and Schröer W., *Adv. Chem. Phys.*, **116** (2001) 1.
[8] Caillol J.-M., Levesque D. and Weis J.-J., *J. Chem. Phys.*, **107** (1977) 1565.
[9] Orkoulas G. and Panagiotopoulos A. Z., *J. Chem. Phys.*, **110** (1999) 1581.
[10] Yan Q. and de Pablo J. J., *J. Chem. Phys.*, **111** (1999) 9509.
[11] Panagiotopoulos A. Z., *J. Chem. Phys.*, **116** (2002) 3007.
[12] Belloni L., *J. Chem. Phys.*, **98** (1993) 8080.
[13] Fisher M. E. and Levin Y., *Phys. Rev. Lett.*, **71** (1993) 3826.
[14] Levin Y. and Fisher M. E., *Physica A*, **225** (1996) 164.
[15] Kalyuzhnyi Yu. V., *Mol. Phys.*, **94** (1998) 735.
[16] Jiang J. W., Blum L. and Bernard O., *Mol. Phys.*, **99** (2001) 1765.
[17] Jiang J. W., Blum L., Bernard O., Prausnitz J. M. and Sandler S. I., *J. Chem. Phys.*, **116** (2002) 7977.
[18] Caillol J.-M. and Weis J.-J., *J. Chem. Phys.*, **102** (1995) 7610.
[19] Bresme F., Lomba E., Weis J.-J. and Abascal J. L. F., *Phys. Rev. E*, **51** (1995) 289.
[20] Shelley J. C. and Patey G. N., *J. Chem. Phys.*, **103** (1995) 8299.
[21] Kalyuzhnyi Yu. V. and Cummings P. T., *J. Chem. Phys.*, **115** (2001) 540.
[22] Kalyuzhnyi Yu. V. and Cummings P. T., *J. Chem. Phys.*, **116** (2002) 8637.
[23] Romero-Enrique J. M., Rull L. F. and Panagiotopoulos A. Z., *Phys. Rev. E*, **66** (2002) 041204.
[24] Sollich P., *J. Phys. Condens. Matter*, **14** (2002) R79.
[25] Bellier-Castella L., Xu H. and Baus M., *J. Chem. Phys.*, **113** (2000) 8337.
[26] Kalyuzhnyi Yu. V. and Kahl G., *J. Chem. Phys.*, **119** (2003) 7335.
[27] Kalyuzhnyi Yu. V., Holovko M. F. and Vlachy V., *J. Stat. Phys.*, **100** (2000) 243.
[28] Kalyuzhnyi Yu. V., Kahl G. and Cummings P. T., *J. Chem. Phys.*, **120** (2004) 10133.
[29] Wilding N. B., Fasolo M. and Sollich P., *J. Chem. Phys.*, **121** (2004) 6887.
[30] Kalyuzhnyi Yu. V., Kahl G. and Cummings P. T., to be published in *J. Chem. Phys.* (2005).
[31] Bernard O. and Blum L., *J. Chem. Phys.*, **104** (1996) 4746.
[32] Bernard O. and Blum L., *J. Chem. Phys.*, **112** (2000) 7227.
[33] Wertheim M. S., *J. Stat. Phys.*, **35** (1984) 19.
[34] Wertheim M. S., *J. Stat. Phys.*, **35** (1984) 35.
[35] Romero-Enrique J. M., Orkoulas G., Panagiotopoulos A. Z. and Fisher M. E., *Phys. Rev. Lett.*, **85** (2000) 4558.
[36] Yan Q. and de Pablo J. J., *J. Chem. Phys.*, **114** (2001) 1727.